



# Line-mixing in the QQ sub branches of the $\nu_1$ band of methyl chloride

Cédric Bray, Ha Tran, David Jacquemart, Nelly Lacome

## ► To cite this version:

Cédric Bray, Ha Tran, David Jacquemart, Nelly Lacome. Line-mixing in the QQ sub branches of the  $\nu_1$  band of methyl chloride. *Journal of Quantitative Spectroscopy and Radiative Transfer*, 2012, 113 (17), pp.2182-2188. 10.1016/j.jqsrt.2012.07.026 . hal-00745984

**HAL Id: hal-00745984**

**<https://hal.sorbonne-universite.fr/hal-00745984>**

Submitted on 26 Oct 2012

**HAL** is a multi-disciplinary open access archive for the deposit and dissemination of scientific research documents, whether they are published or not. The documents may come from teaching and research institutions in France or abroad, or from public or private research centers.

L'archive ouverte pluridisciplinaire **HAL**, est destinée au dépôt et à la diffusion de documents scientifiques de niveau recherche, publiés ou non, émanant des établissements d'enseignement et de recherche français ou étrangers, des laboratoires publics ou privés.

# Line-mixing in the $^oQ$ sub branches of the $\nu_1$ band of methyl chloride

*C. Bray<sup>a,b,\*</sup>, H. Tran<sup>c</sup>, D. Jacquemart<sup>a,b</sup>, N. Lacome<sup>a,b</sup>*

<sup>a</sup>UPMC Univ Paris 06, Laboratoire de Dynamique, Interactions et Réactivité, UMR 7075,  
Case Courrier 49, 4 Place Jussieu, 75252 Paris Cedex 05, France

<sup>b</sup>CNRS, UMR 7075, Laboratoire de Dynamique, Interactions et Réactivité, Case Courrier 49,  
4 Place Jussieu, 75252 Paris Cedex 05, France

<sup>c</sup>Laboratoire Interuniversitaire des Systèmes Atmosphériques, UMR CNRS 7583, Université  
Paris Est Créteil (UPEC) et Université Paris Diderot (UPD). Université Paris Est Créteil, 61  
avenue du Général de Gaulle, 94010 Créteil Cedex, France

Number of Figures: 5

Number of Tables: 3

Please send proofs to: Bray Cédric

\* corresponding author : Cédric Bray (Email: [bray@spmol.jussieu.fr](mailto:bray@spmol.jussieu.fr))

Tel. 33 (0)1 44 27 36 82 - Fax: 33 (0)1 44 27 30 21

Keywords : methyl chloride;  $\nu_1$  band; High-resolution Fourier Transform spectra; room  
temperature; line-mixing; vibration rotation.

## Abstract

Line-mixing effects have been studied in the  $\nu_1 \ ^Q Q_K$  ( $K$  from 0 to 10) sub branches of methyl chloride ( $\text{CH}_3\text{Cl}$ ) perturbed by nitrogen ( $\text{N}_2$ ). Laboratory Fourier transform spectra have been recorded at room temperature for various pressures of atmospheric interest. In order to accurately model these spectra, a theoretical approach accounting for line-mixing effects is necessary and proposed in this study. The common model used in this work is based on the state-to-state rotational cross-sections calculated by a statistical modified exponential-gap fitting law depending on few empirical parameters. These parameters have been deduced by least-squares fitting a sum rule to the  $\text{N}_2$ -broadening coefficients modeled previously. Comparisons between experimental and calculated spectra for various  $\ ^Q Q$  sub branches and various pressures of  $\text{N}_2$  demonstrate the adequacy of the model as compared to the use of the Voigt profile.

## 1. Introduction

Methyl chloride ( $\text{CH}_3\text{Cl}$ ) is one of the most abundant chlorine-containing molecules in the earth atmosphere. It has a rather strong signature around  $3000\text{ cm}^{-1}$  (especially the  $\nu_1$  band) which was recently used by the Atmospheric Chemistry Experiment (ACE) satellite mission to produce the first global distribution of methyl chloride in the upper troposphere and stratosphere [1]. This spectral region has been recently studied, for transitions of both  $\text{CH}_3^{35}\text{Cl}$  and  $\text{CH}_3^{37}\text{Cl}$  isotopologues, in terms of line positions and intensities [2], self- [3] and  $\text{N}_2$ -broadening coefficients [4].

$^Q Q$  sub branches of the  $\nu_1$  band are used for atmospheric remote sensing in this region since they are quite strong and in a relatively transparent window. Under atmospheric conditions, line-mixing effects can be observed since the structure of these branches is narrow [5]. In the following, it is shown that the line mixing effects in the  $^Q Q$  sub branches must be taken into account for accurate atmospheric applications. Line-mixing effects were disregarded in our previous studies [2-4], since low pressures of  $\text{CH}_3\text{Cl}$  or  $\text{N}_2$  (lower than 120 mbar) spectra were used. In the present work, nitrogen ( $\text{N}_2$ ) pressures up to 700 mbar are considered. In such conditions, the usual Voigt or Lorentz profiles cannot correctly reproduce the experimental shape of the  $^Q Q$  sub branches. Note that, for  $\text{CH}_3\text{Cl}$ , line-mixing has been previously studied for the  $^R Q_0$  sub-branches of the  $\nu_5$  band [6-8], but never for the  $\nu_1$  band. In this work, a model has been used to calculate line-mixing for the  $^Q Q_K$  ( $K$  from 0 to 10) sub-branches of the  $\nu_1$  band of  $\text{CH}_3\text{Cl}$  perturbed by  $\text{N}_2$ . This model is based on the use of the state-to-state rotational cross-sections and a statistical Exponential Power Gap (EPG) fitting law depending on few empirical parameters.

Laboratory Fourier transform spectra have been recorded at room temperature and for 3 pressures of  $\text{N}_2$  (between 200 and 700 mbar). Line mixing effects are observed in the  $^Q Q$  sub-branches, and increased with the pressure of  $\text{N}_2$ . Experimental conditions are presented in Section 2. Section 3 is devoted to the line mixing model. Comparisons between experimental and calculated spectra are discussed in Section 4.

## 2. Experimental conditions

The rapid scan Bruker IFS 120 HR interferometer of the Laboratoire de Dynamique, Interactions et Réactivité (LADIR) was used to record  $\text{N}_2$ -perturbed spectra of  $\text{CH}_3\text{Cl}$ . The

unapodized spectral resolution (FWHM) used was about  $25 \times 10^{-3} \text{ cm}^{-1}$ , corresponding to a maximum optical path difference of 20 cm. Such a resolution is sufficient enough to neglect the apparatus function in the calculation because of the strong width (around  $0.2 \text{ cm}^{-1}$  at 1 atm of  $\text{N}_2$ ) of the  $^Q Q$  sub branches of  $\text{CH}_3\text{Cl}$ . The interferometer was equipped with a  $\text{CaF}_2$  beamsplitter, an InSb detector and a Globar source. The experimental conditions of the recorded spectra are summarized in Table 1. Under these conditions, the rotational structure of  $\text{CH}_3\text{Cl}$  transitions is not resolved, as can be observed in Fig. 1, which presents the various  $^Q Q$  sub branches studied in this work. For all spectra, the whole optical path was under vacuum. A multipass cell of 1m base length, with a total absorption path of 415 cm, was used. This cell was equipped with KCl windows. The commercial gas sample of  $\text{CH}_3\text{Cl}$  and  $\text{N}_2$ , furnished by Alpha gas with a stated purity of 99.9% in natural abundances (74.89 % of  $^{12}\text{CH}_3^{35}\text{Cl}$  and 23.94 % of  $^{12}\text{CH}_3^{37}\text{Cl}$ ), was used without further purification. The temperature in the cell was recorded using four platinum probes inside the cell. The spectra were recorded at room temperature (see Table 1). Pressures of gases have been measured with two Baratron gauges with accuracy better than  $\pm 0.15 \%$  for the 1 mbar full scale gauge and better than  $\pm 0.25 \%$  for the 1000 mbar full scale gauge. Around 400 scans have been averaged and then transformed to spectrum, using the Fourier transform procedure included in the Bruker software OPUS package [9], selecting a Mertz phase-error correction [10,11]. The spectra were not numerically apodized. Averaging the 400 scans, the signal-to-noise ratio was nearly equal to 600. Note that, a weak multiplicative channel spectrum was expected in the experimental spectra due to the reflexion on parallel faces of windows in the experimental set up (1% maximum peak to peak amplitude). Due to the high pressures of gas used in this work, this channel cannot be observed in the spectral range of the  $\text{CH}_3\text{Cl}$  absorption features. In this study, the pressure broadening width leads to intrinsic non resolved transitions, especially for the  $^Q Q$  sub branches, so that, the multiplicative channel was hidden behind. Consequently, spectra were divided by a vacuum spectrum to eliminate this channel.

### 3. Line-mixing calculation

This section is dedicated to the calculation used to evaluate line-mixing effects in  $\text{CH}_3\text{Cl}/\text{N}_2$  spectra for  $^Q Q$  sub-branches of  $\nu_1$  band. Sections 3.1 and 3.2 are devoted to the formulation of the absorption coefficient and of the relaxation operator respectively. The calculation of  $\text{CH}_3\text{Cl}$  spectra perturbed by  $\text{N}_2$  under the experimental conditions given in Table 1 is described in Section 3.3.

### 3.1. Absorption coefficient

Let us consider a mixture of two gases, an absorbing gas (noted  $a$ ) and a buffer gas (noted  $b$ ). Within the impact and binary collisions approximations, and disregarding Doppler effect, which has negligible influences in the studied pressure range, the absorption coefficient  $\alpha$  (in  $\text{cm}^{-1}$ ) accounting for line-mixing effects at a wavenumber  $\sigma$  is given by [12,13] (Note that the CGS unit system is used for all the quoted equations):

$$\alpha(\sigma, P_a, P_b, T) = \frac{8\pi^2\sigma}{3hc} [1 - \exp(-hc\sigma / k_b T)] P_a \sum_k \sum_l \rho_k(T) d_k d_l \times \text{Im} \left\langle \left\langle l \left[ \Sigma - L_0 - i(P_a W_{a/a}(T) + P_b W_{a/b}(T)) \right]^{-1} \right| k \right\rangle \right\rangle, \quad (1)$$

(rajouter {} après Im)

where  $P_a$  and  $P_b$  are the partial pressures of the absorbing and buffer gases, respectively, and  $T$  the temperature of the gas. The sums include all absorption lines  $k$  and  $l$ ;  $\text{Im}\{\dots\}$  denotes the imaginary part;  $\rho_k$  is the relative population of the initial level of line  $k$ ,  $d_n$  is the reduced matrix element of the electric dipole moment operator of line  $n$  ( $n = l$  or  $k$ ), related to the integrated line intensity  $S_n$  of the absorbing gas by:

$$S_n(T) = \frac{8\pi^3}{3hc} \rho_n(T) \sigma_n [1 - \exp(hc\sigma_n / k_b T)] d_n^2. \quad (2)$$

$k_b$  is the constant of Boltzmann.  $\Sigma$ ,  $L_0$  and  $W$  are operators in the Liouville line space. The first two are diagonal and can be expressed as follows:

$$\langle \langle l | \Sigma | k \rangle \rangle = \sigma \delta_{k,l} \quad \text{and} \quad \langle \langle l | L_0 | k \rangle \rangle = \sigma_k \delta_{k,l}, \quad (3)$$

$\delta_{k,l}$  being the Kronecker symbol. The relaxation operators  $W_{a/a}$  and  $W_{a/b}$ , which contain the influence of collisions on the spectral shape, depend on the band and on the temperature. The off-diagonal elements of  $W$  account for interferences between absorption lines (line mixing), whereas the real and imaginary parts of the diagonal elements are the pressure-broadening  $\gamma_k$  and pressure-shifting coefficients  $\delta_k$  of the lines

$$\langle \langle k | W(T) | k \rangle \rangle = \gamma_k(T) - i\delta_k(T). \quad (4)$$

### 3.2. Relaxation operator

According to Eq. (4), the diagonal elements of  $W$  are directly linked to the broadening and shifting coefficients of the transitions involved in line mixing calculation. Since no  $N_2$  shifting coefficient of  $CH_3Cl$  is available in this region, they have been neglected in this study. Therefore, the imaginary part of the off-diagonal elements has also been disregarded.

The real off-diagonal elements are modeled using the state-to-state inelastic collisional rates of the lower state through:

$$\langle\langle l|W(T)|k\rangle\rangle = -A_{l,k}K(i_l \leftarrow i_k, T) \text{ with } (i_l \neq i_k), \quad (5)$$

where  $K(i_l \leftarrow i_k, T)$  designates the state-to-state collisional transfer rate from the initial level  $i_k$  of line  $k$  to the initial level  $i_l$  of line  $l$ . The parameters  $A_{l,k}$ , which enable switching from the state space to the line space, are empirical and depend on the types of considered lines [14,15]. In order to simplify the problem, we made the approximation that  $A_{l,k}$  depends only on the band and on the buffer gas, but not on the quantum numbers of the lines themselves.

The downward rates  $K(i_l \leftarrow i_k, T)$ , with  $E_l < E_k$ , are modeled by a statistical Exponential Power Gap (EPG) fitting law [10,13,16]:

$$K(i_l \leftarrow i_k, T) = a_1 |E_k - E_l|^{-a_2} e^{-a_3 |E_k - E_l|}, \quad (6)$$

where  $E_n$  is the rotational energy of the initial level of line  $n$  ( $n = l$  or  $k$ ). The coefficients  $a_1$ ,  $a_2$  and  $a_3$  are empirical parameters.

The upward rates are then calculated by using the detailed balance:

$$K(i_k \leftarrow i_l, T) = \frac{\rho_k(T)}{\rho_l(T)} K(i_l \leftarrow i_k, T). \quad (7)$$

The coefficients  $a_1$ ,  $a_2$  and  $a_3$  in Eq. (6) are obtained by least-squares fitting the sum rule to the N<sub>2</sub>-broadening coefficients  $\gamma_k$  values. For a  $^Q Q$  sub branch, this sum rule is given by:

$$\gamma_k = \frac{1}{2} \left[ \sum_{i_k \neq i_l} K(i_l \leftarrow i_k) + \sum_{f_k \neq f_l} K(f_l \leftarrow f_k) \right], \quad (8)$$

where  $i_n$  and  $f_n$  are, respectively, the initial and final levels of the transition  $n$  ( $n = l$  ou  $k$ ).

### 3.3. Application to the CH<sub>3</sub>Cl spectra

Using experimental conditions of Table 1 and the model previously described, the line mixing due to N<sub>2</sub> pressure has been calculated in the various  $^Q Q_K$  ( $K$  from 0 to 10) sub branches of the  $\nu_1$  band. As theses  $^Q Q$  sub branches are well separated (see Fig. 1), inter-branch line mixing (for example with  $\Delta K=3n$  [17]) has not been taken into account.

The spectroscopic parameters of the line  $k$  required for the calculation of the spectra are the position  $\sigma_k$ , the relative population of the initial level  $\rho_k$ , the reduced matrix element of the electric dipole moment operator  $d_k$  (obtained from  $S_k$ ), the rotational energy level  $E_k$ ,

and the N<sub>2</sub>-broadening coefficients  $\gamma_k$ . All these parameters have been constrained to the calculated values obtained in Refs. [2-4]. Since partial pressure of methyl chloride is very small (around 0.25 mbar), self-broadening contribution has been neglected. The contributions of the <sup>13</sup>C species (concentration of about 1%) were also neglected. Note that the whole absorption coefficient is the sum of the absorption coefficients due to each isotopologues and that the line intensity in Eq. (2) is defined for a pure gas, not to be confused with those given in natural abundances in Ref. [2].

For the calculation of the off-diagonal elements of the relaxation operators  $W_{CH_3Cl/N_2}$ , the parameters  $a_1$ ,  $a_2$  and  $a_3$  have been adjusted using Eq. (6), the calculated N<sub>2</sub>-broadening coefficients of Ref. [4], and the sum rule given in Eq. (8). For this, the values of the broadening coefficients obtained by an empirical model in Ref. [4] were chosen, instead of the measured values. The N<sub>2</sub>-broadening coefficients have been calculated with the empirical model of Ref. [4] from  $J$  equal 0 to 50 and  $K$  equal 0 to 9. Since in Ref. [4] no evident discrepancy has been observed between the N<sub>2</sub>-broadening coefficients of CH<sub>3</sub><sup>35</sup>Cl and CH<sub>3</sub><sup>37</sup>Cl, the  $a_1$ ,  $a_2$  and  $a_3$  parameters are the same for both isotopologues. The parameters  $a_1$ ,  $a_2$  and  $a_3$  have been obtained for the most intense  $^oQ_6$  sub branch, and were retained for all the other  $^oQ$  sub branches.

The vibrational ground state has only A+ levels. The upper states of  $^oQ_6$  transitions are split into A- and A+ levels. The optical selection rule for these  $^oQ_6$  transitions is A+ $\leftrightarrow$ A-. As mentioned by Chackerian et al. [8], collisional relaxation between both A- $\leftrightarrow$ A- and A+ $\leftrightarrow$ A- levels (instead of only A- $\leftrightarrow$ A-) in the excited state were needed to correctly describe line-mixing effects in the  $^RQ_0$  sub branch of the  $\nu_5$  band of CH<sub>3</sub>Cl. In this case, the sum rule becomes:

$$\gamma_k = \frac{1}{2} \left[ \sum_{i_k \neq i_l} K(i_l \leftarrow i_k) + \frac{1}{2} \sum_{\substack{f_k \neq f_l \\ A \leftrightarrow A+}} K(f_l \leftarrow f_k) + \frac{1}{2} \sum_{\substack{f_k \neq f_l \\ A \leftrightarrow A-}} K(f_l \leftarrow f_k) \right]. \quad (9)$$

However, in the case of the  $^oQ$  sub branch of the  $\nu_1$  band of CH<sub>3</sub>Cl, the rotational energies of A- and A+ levels of the upper state are very close, so that this refinement does not change the value of the right member of Eq. (8). Therefore, only A- $\rightarrow$ A- collisional relaxations in the upper state have been considered to simplify the calculation. Consequently Eq. (9) becomes:

$$\gamma_k = \frac{1}{2} \left[ \sum_{i_k \neq i_l} K(i_l \leftarrow i_k) + \sum_{\substack{f_k \neq f_l \\ A \leftrightarrow A-}} K(f_l \leftarrow f_k) \right]. \quad (10)$$



For the  ${}^oQ_6$  sub-branch, the sum rule was evaluated with unrestricted collisional selection rules on  $\Delta J$ , with  $J_k$  of the lower state lesser or equal to 35 and with  $J_l$  of the upper state up to 50 (in order to ensure the convergence of the rule sum [Eq. (10)]) and with  $\Delta K = 0$  [17,19-21].

The values obtained for the  $a_1$ ,  $a_2$ , and  $a_3$  coefficients are given in Table 2, and the validity of the model is demonstrated in Fig. 2, showing the comparison between the  $N_2$ -broadening coefficients calculated in such a way and the values from Ref. [4]. The coefficient  $A_{l,k}$  in Eq. (5) was determined from one single experimental spectrum (spectre 3 of Table 1). This was done by successive estimations, and we found that the coefficient  $A_{N_2} = 0.55$  was the optimum value to reproduce both sub branches at the three experimental pressures. For all  ${}^oQ$  sub branches, the relaxation operators  $W_{CH_3Cl/N_2}$  were then calculated from the set of parameters of Table 2, using Eqs. (5-7) and using the parameter  $A_{N_2}$ . The broadening parameters calculated from the off-diagonal elements and the sum rule does not match perfectly (see Fig. 2) especially for the other  ${}^oQ$  sub branches for which the broadening coefficients for  $K=6$  differs from those at other  $K$  values. Consequently a renormalization procedure [18] was applied to the off-diagonal terms for each branch, in order to satisfy exactly the sum rule and the  $K$  rotational dependence of the  $N_2$ -broadening coefficients. Finally, note that the calculation of spectra was performed by the direct calculation of Eq. (1) through the inversion of the relaxation operators  $W_{CH_3Cl/N_2}$ .

#### 4. Spectra calculations and discussion

Due to the broadened unresolved structure of the  ${}^oQ$  branches (about  $0.2 \text{ cm}^{-1}$  at 1 atm), it was not necessary to take into account the effect of apparatus function. Absorption coefficients due to the two  $CH_3^{35}Cl$  and  $CH_3^{37}Cl$  isotopologues were added. Uncoupled lines present in the studied spectral domains were also taken into account in the calculation of the total absorption coefficient, their contribution being calculated using a Lorentz profile. Because of the high pressures, it was not necessary to take into account the Doppler broadening for  $CH_3Cl$  in this spectral region. Moreover, due to the low pressures of  $CH_3Cl$  used in this work, the effect of the self-broadening coefficients has been neglected. In the studied spectral region, the Doppler width is about  $0.0025 \text{ cm}^{-1}$ , whereas in spectrum 1 (see table 1) the self-width is equal to  $0.0002 \text{ cm}^{-1}$ , while the  $N_2$ -width is equal to  $0.04 \text{ cm}^{-1}$ .

Using the  $a_1$ ,  $a_2$ , and  $a_3$  parameters reported in Table 2 for  $N_2$ -perturbed  $CH_3Cl$  and the value  $A_{N_2} = 0.55$ , calculation with and without line mixing effect were performed. The results obtained for the  $^oQ_6$  sub branches at the three pressures of Table 1 are presented in Fig. 3. The residuals can achieve 30% when not introducing line-mixing effects, whereas it achieved only 6% when taking this effect into account with our model. The spectra calculated for the other  $^oQ$  sub branches are shown in Fig. 4. Let us recall that the renormalization procedure was necessary for these branches, since the model parameters were obtained from the  $^oQ_6$  sub branch only. As can be observed in Fig. 4, line-mixing effects are quite important for all sub branches and our calculation significantly improves the residual as compared to a calculation without line mixing. Table 3 shows the maximum residual in percent for each branch when performing line mixing calculation or using a Lorentz profile. A slight systematic residual increasing with  $K$  is observed. This difference can be due to a  $K$  dependence of line-mixing effects not introduced in our  $W_{CH_3Cl/N_2}$  calculation since the  $A$  coefficient is constant for all  $^oQ$  sub branches, and to the fact that  $N_2$  pressure-shift has been neglected. For branches with high  $K$  values ( $K > 8$ ), less accurate spectroscopic data can also explain the more important residual. These results confirm that neglecting line mixing leads to large errors, whereas our model gives better predictions.

A comparison between a calculated spectrum based on the line parameters of Refs. [2-4] and the experimental spectrum of the Pacific Northwest National Laboratory (PNNL) [22] is shown in Fig. 5. The PNNL spectrum was recorded at 0.001 mbar of  $CH_3Cl$  and 1013 mbar of  $N_2$ . Under these conditions, the calculated spectrum presents strong effect of line mixing as it can be observed on this figure. The improvement on the calculation when the line mixing is taking into account is significant. For atmospheric retrievals from the  $^oQ$  sub branches of the  $\nu_1$  band of  $CH_3Cl$ , the use of line parameters from databases [23-24] or from Refs. [2-4] is not sufficient since neglecting line-mixing effects will introduce systematic errors in the retrieval of the  $CH_3Cl$  abundance.

## 5. Conclusion

Line-mixing effects have been calculated for the  $^oQ$  sub branches (up to  $K = 10$ ) of the  $\nu_1$  band of methyl chloride ( $CH_3Cl$ ), perturbed by  $N_2$  (200-700 mbar) at room temperature. The model is based on the use of the state-to-state rotational cross-sections calculated by a statistical modified exponential-gap fitting law that depends on a few adjusted empirical parameters. Comparisons performed between experimental and calculated spectra

demonstrate the effectiveness of the model as compared to the use of a Voigt or Lorentz profile. The influence of line-mixing effects on the abundance of  $\text{CH}_3\text{Cl}$  is important for atmospheric retrievals. All programs and results that are required to calculate the line mixing for  $^Q$  sub branches of the  $\nu_1$  band of  $\text{CH}_3\text{Cl}$  are available upon request to the authors.

#### Acknowledgments

Dr. J.-M. Hartmann and Dr. A. Perrin are gratefully acknowledged for very helpful suggestions and discussions throughout this work.

## References

- [1] Kaley AW, Weigum N, McElcheran C, Taylor JR. Global methyl chloride measurements from the ACE-FTS instrument. International Symposium on Molecular Spectroscopy Department of Chemistry The Ohio State University, TI-09; 2009.
- [2] Bray C, Perrin A, Jacquemart D, Lacome N. The  $\nu_1$ ,  $\nu_4$  and  $3\nu_6$  bands of methyl chloride in the 3.4  $\mu\text{m}$  region: line positions and intensities. JQSRT 2011;112:2446-62.
- [3] Bray C, Jacquemart D, Lacome N, Guinet M, Cuisset A, Eliet S, Hindle F, Mouret G, Rohart F, Buldyreva J. Self-broadening coefficients of methyl chloride transitions at room temperature. Submitted in JQSRT.
- [4] Bray C, Jacquemart D, Buldyreva J, Lacome N, Perrin A. The  $\text{N}_2$ -broadening coefficients of methyl chloride at room temperature. JQSRT 2012;113:1102-12.
- [5] Hartmann JM, Boulet C, Robert D. Collisional effects on molecular spectra. Elsevier; 2008.
- [6] Hartmann JM, Bouanich JP, Boulet C, Blanquet G, Walrand J, Lacome N. Simple modelling of  $Q$  branch absorption-II: application to molecules of atmospheric interest (CFC-22 and  $\text{CH}_3\text{Cl}$ ). JQSRT 1995;54:723–35.
- [7] Frichot F, Lacome N, Hartmann JM. Pressure and temperature dependences of absorption in the  $\nu_5$   $^RQ_0$  branch of  $\text{CH}_3\text{Cl}$  in  $\text{N}_2$ : measurements and modelling. J Mol Spectrosc 1996;178:52-8.
- [8] Chackerian Jr. C, Brown LR, Lacome N, Tarrago G. Methyl chloride  $\nu_5$  region lineshape parameters and rotational constants for the  $\nu_2$ ,  $\nu_5$ , and  $2\nu_3$  vibrational bands. J Mol Spectrosc 1998;191:148-57.
- [9] Wartewig S. IR and Raman spectroscopy: fundamental processing. Weinheim: Wiley-VCH; 2003.
- [10] Mertz L. Transformations in optics. New York: Wiley; 1965.
- [11] Griffiths PR, deHaseth JA. Fourier transform infrared spectrometry. New York: Wiley; 1986.
- [12] Ben-Reuven A. Impact broadening of microwave spectra. Phys Rev 1966;145:7-22.
- [13] Lévy A, Lacome N, Chackerian Jr. C. Collisional line-mixing. In: Rao KN, Weber A, editors. Spectroscopy of the Earth's atmosphere and interstellar medium. New York: Academic Press, Inc.; 1992. p. 261-337.
- [14] Pieroni D, Nguyen Van T, Brodbeck C, Claveau C, Valentin A, Hartmann JM, et al. Experimental and theoretical study of line-mixing in methane spectra. I. The  $\text{N}_2$ -broadened  $\nu_3$  band at room temperature. JQSRT 1999;110:7717-32.

- [15] Tran H, Flaud PM, Gabard T, Hase F, von Clarmann T, Camy-Peyret C, Payan S, Hartmann JM. Model, software and database for line-mixing effects in the  $\nu_3$  and  $\nu_4$  bands of  $\text{CH}_4$  and tests using laboratory and planetary measurements-I:  $\text{N}_2$  (and air) broadening and the Earth atmosphere. *JQSRT* 2006;101:284–305.
- [16] Rahn LA, Palmer RE. Studies of nitrogen self-broadening at high temperature with inverse Raman spectroscopy. *J Opt Soc Am B* 1986;3:1164–9.
- [17] Herlemont F, Thibault J, Lemaire J. Study of rotational relaxation in  $\text{CH}_3\text{Br}$  by infrared–microwave double resonance. *Chem Phys Lett* 1976;41:466–9.
- [18] Niro F, Boulet C, Hartmann JM. Spectra calculations in central and wing region of  $\text{CO}_2$  IR bands between 10 and 20 mm-I: model and laboratory measurements. *JQSRT* 2004;88:483–98.
- [19] Everitt HO, de Lucia F. Rotational energy transfer in  $\text{CH}_3\text{F}$ : the  $\Delta J=n$ ,  $\Delta f=0$  processes. *J Chem Phys* 1990;92:6480–91.
- [20] Frenkel L, Marantz H, Sullivan T. Spectroscopy and collisional transfer in  $\text{CH}_3\text{Cl}$  by microwave–laser double resonance. *Phys Rev A* 1971;3:1640–51.
- [21] Pape TW, De Lucia FC, Skatrud DD. Time resolved double resonance study of  $J$  and  $K$  changing rotational collision processes in  $\text{CH}_3\text{Cl}$ . *J Chem Phys* 1994;100:5666–83.
- [22] Sharpe SW, Johnson TJ, Sams RL, Chu PM, Rhoderick GC, Johnson PA. Gas-Phase Databases for Quantitative Infrared Spectroscopy. *Appl Spectrosc* 2004; 58:1452–61.
- [23] Rothman LS, Gordon IE, Barbe A, Benner DC, Bernath PF, Birk M, Boudon V, Brown LR, Campargue A, Champion JP, Chance K, Coudert LH, Dana V, Devi VM, Fally S, Flaud JM, Gamache RR, Goldman A, Jacquemart D, Kleiner I, Lacombe N, Lafferty QJ, Mandin JY, Massie ST, Mikhailenko SN, Miller CE, Moazzen-Ahmadi N, Naumenko OV, Nikitin AV, Orphal J, Perevalov VI, Perrin A, Predoi-Cross A, Rinsland CP, Rotger M, Simeckova M, Smith MAH, Sung K, Tashkun SA, Tennyson J, Toth RA, Vandaele AC, Vander Auwera J. The HITRAN 2008 molecular spectroscopic database. *JQSRT* 2009;110:533–72.
- [24] Jacquinet-Husson N, Scott NA, Chédin A, Crépeau L, Armante R, Capelle V, Orphal J, Coustenis A, Barbe A, M. Birk, Brown LR, Camy-Peyret C, Claveau C, Chance K, Christidis N, Clerbaux C, Coheur PF, Dana V, Daumont L, Debacker-Barilly MR, Di Lonardo G, Flaud JM, Goldman A, Hamdouni A, Hess M, Hurley MD, Jacquemart D, Kleiner I, Köpke P, Mandin JY, Massie S, Mikhailenko S, Nemtchinov V, Nikitin A, Newnham D, Perrin A, Perevalov VI, Pinnock S, Régalia-Jarlot L, Rinsland CP, Rublev A, Schreier F, Schult L, Smith KM, Tashkun SA, Teffo JL, Toth RA, Tyuterev VI, Vander Auwera J, Varanasi P, Wagner G, The GEISA spectroscopic database: Current and future archive for Earth’s planetary atmosphere studies. *JQSRT* 2008;109:1043–59.

**Table 1**

Experimental conditions of the recorded spectra.

#	CH <sub>3</sub> Cl pressure (mbar)	N <sub>2</sub> pressure (mbar)	Resolution <sup>a</sup> (cm <sup>-1</sup> )	Temperature (K)
1	0.2562	218.6	0.02	294.3 ±0.5
2	0.2706	409.8	0.05	293.5 ±0.5
3	0.2640	698.2	0.05	297.0 ±0.5

<sup>a</sup> Resolution as defined by Bruker = 0.9/Maximum optical path

Table 2

Parameters of the EPG model (Eq. 7) obtained for CH<sub>3</sub>Cl/N<sub>2</sub>.

EPG law parameter	CH <sub>3</sub> Cl/N <sub>2</sub>
$a_1$	0.067
$a_2$	0.584
$a_3$	0.764

Table 3

Residual in percent for each branch when line mixing is taken or not into account for the spectrum 3.

Branch of $\nu_1$ band	Obs-calc* Without line mixing (%)	Obs-calc* With line mixing (%)
${}^oQ_1$	-10.6	-0.9
${}^oQ_2$	-21.4	-1.5
${}^oQ_3$	-27.7	5.1
${}^oQ_4$	-29.3	4.4
${}^oQ_5$	-34.0	-1.2
${}^oQ_6$	-29.1	-5.6
${}^oQ_7$	-37.9	-9.1
${}^oQ_8$	-36.5	-9.2
${}^oQ_9$	-35.8	-18.5
${}^oQ_{10}$	-37.3	-18.7

\* Difference at the maximum peak absorption ( % =  $\frac{T_{obs} - T_{calc}}{1 - T_{obs}} \times 100$  ,  $T_{obs}$  and  $T_{calc}$  correspond to the transmittance of the experimental and calculated spectra, respectively)



Figure 1

On left side, in the upper panel, the experimental spectrum 1 (see Table 1) is plotted. The panels of residuals show the differences between the experimental spectrum and a spectrum calculated without taking into account line-mixing (a) and with line mixing taken into account (b). On right side, a zoom of the  $^oQ$  sub branches is plotted.  $K$ -rotational structure of sub branches is resolved contrary to the  $J$ -rotational structure of each branch. Note also that the  $^oQ$  sub branches of the two isotopologues of  $^{12}\text{CH}_3\text{Cl}$  are not resolved.

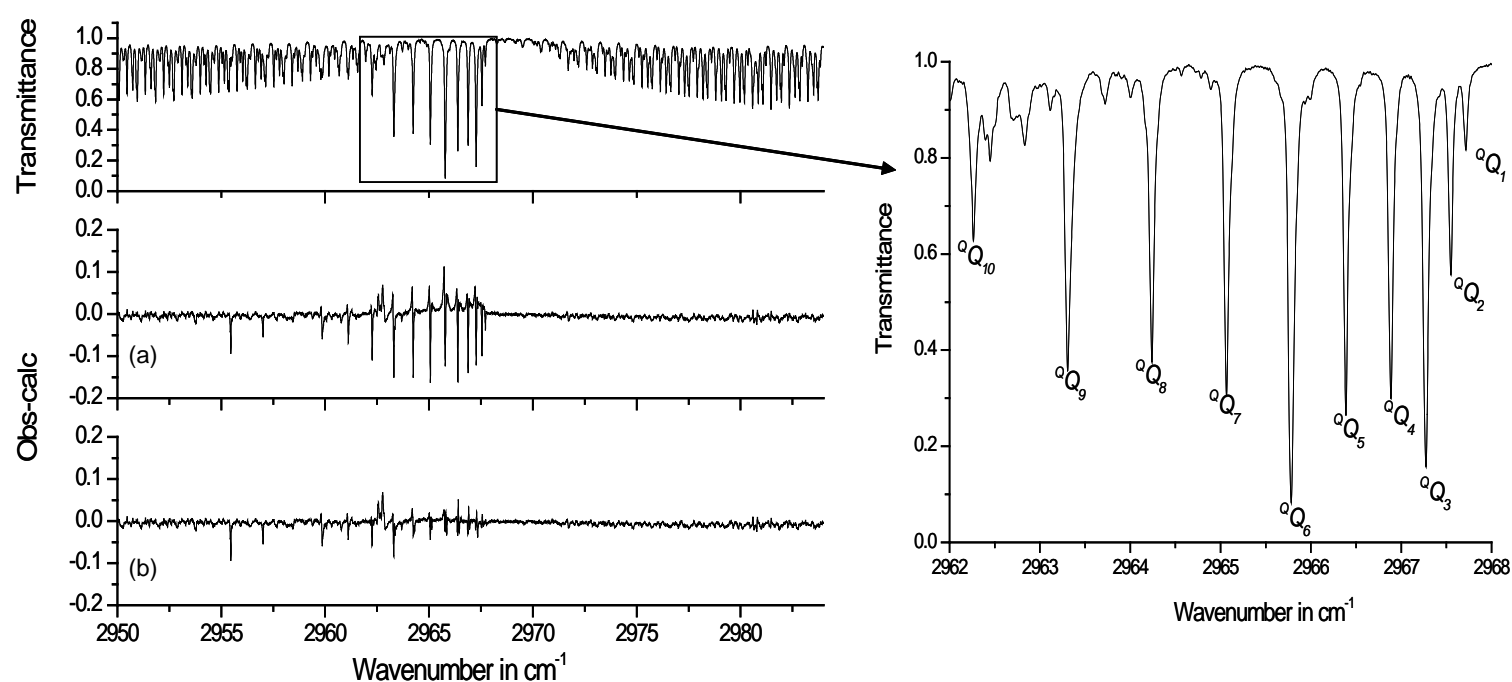


Figure 2

Comparison between N<sub>2</sub>-broadening coefficients of CH<sub>3</sub>Cl in the  $^oQ_6$  sub branch given by the empirical model of [4] (solid square) and those calculated using the EPG model and coefficients of Table 2 (solid curve). Note that the broadening coefficients calculated for CH<sub>3</sub><sup>35</sup>Cl and CH<sub>3</sub><sup>37</sup>Cl are not distinguishable from the solid curve shown.  $J$  is the rotational quantum number of the lower level of the transition.

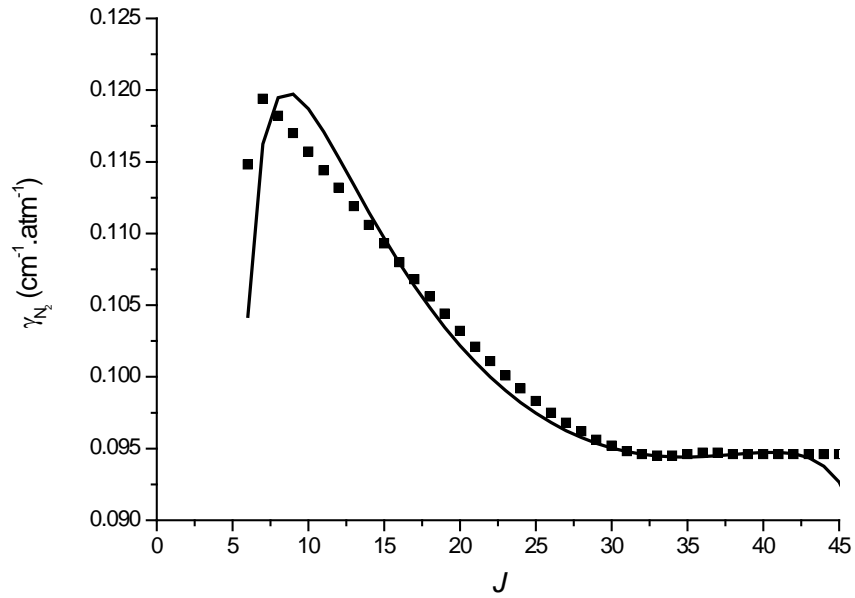
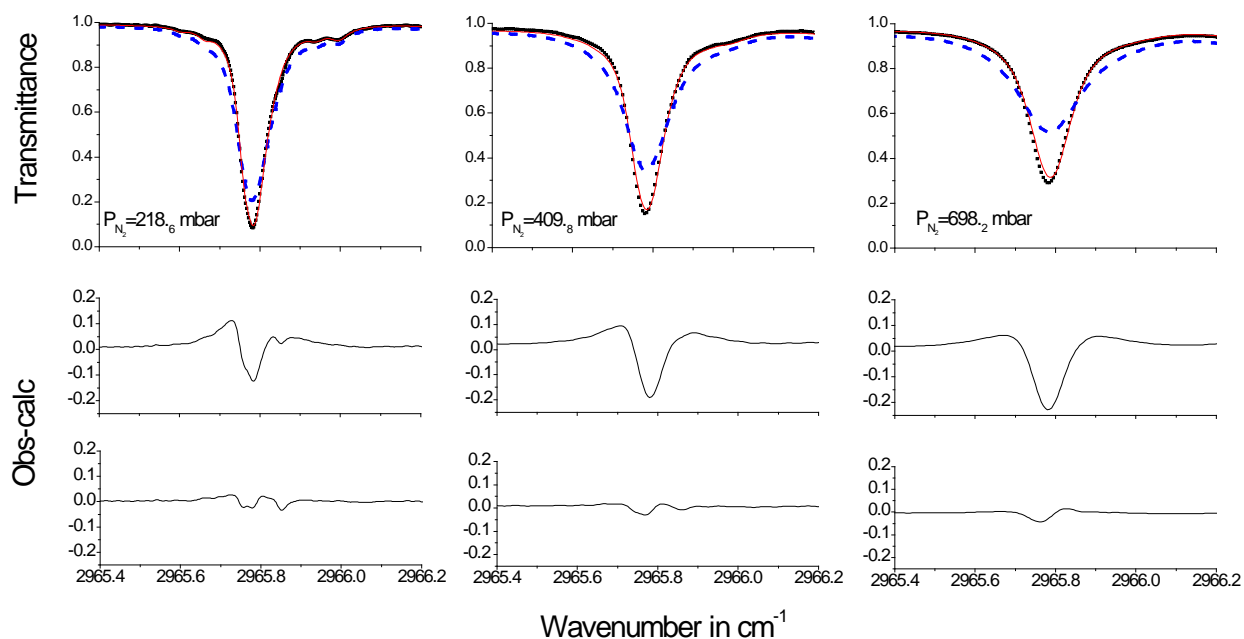


Figure 3

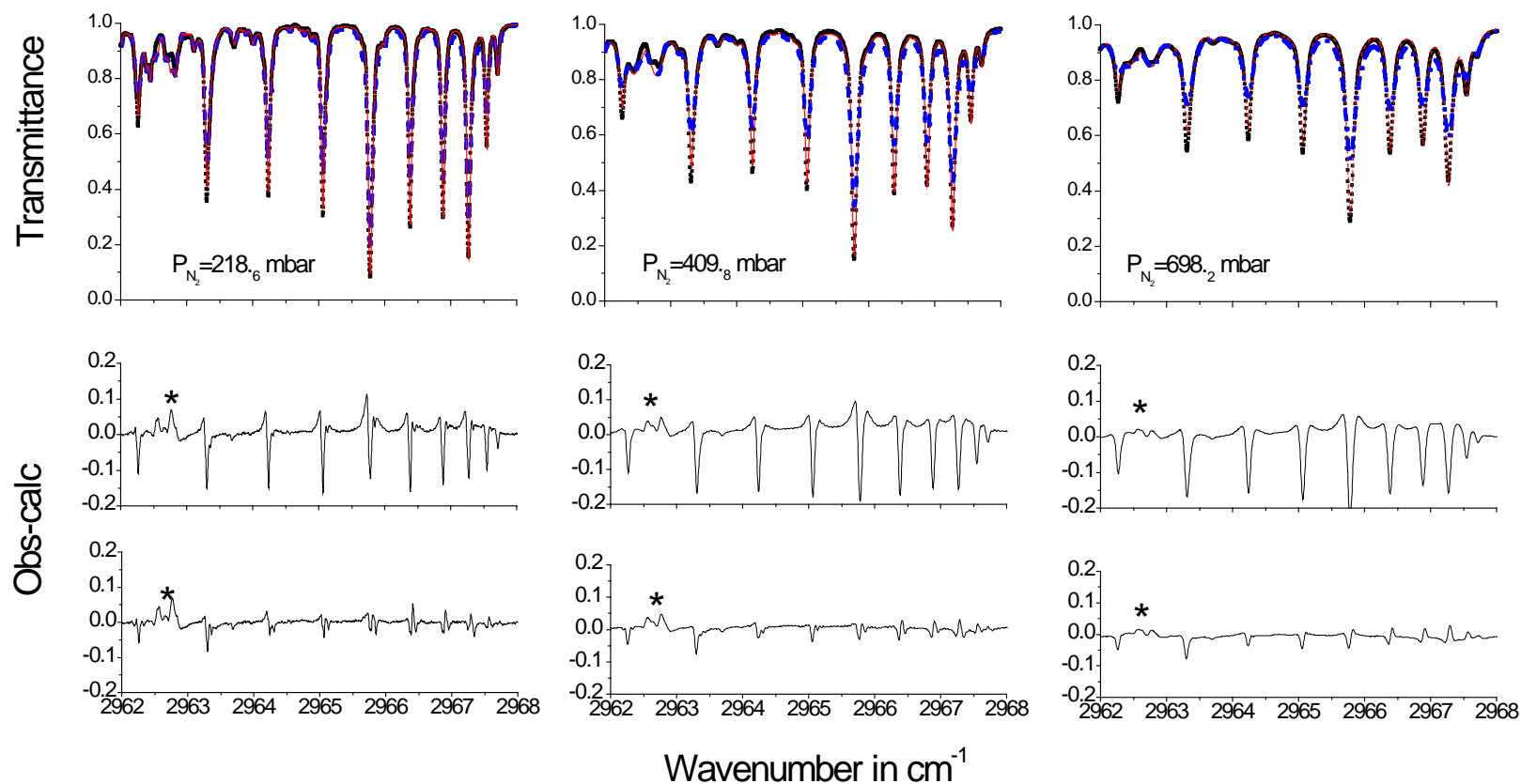
Comparison between the  $\text{CH}_3\text{Cl}/\text{N}_2$  experimental spectra (■) of the  $^oQ_6$  sub-branch and those calculated without line mixing (---), with line mixing (—). The pressure of  $\text{N}_2$  gas increases from left panel to the right one. The lower panels correspond to residuals of the fits showing the differences between the experimental spectra and calculated one using a sum of Lorentz profiles with (last panel) or without (first residual panel) taking into account line-mixing effects.



\*  $\nu_4$  and  $3\nu_6$  transitions taken into account in the calculation of the total absorption coefficient (Lorentz profiles). Spectroscopic data of these transitions are less accurate than the  $\nu_1$  ones.

Figure 4

Comparison between the  $\text{CH}_3\text{Cl}/\text{N}_2$  transmission spectra in the  $^oQ$  sub-branches region calculated without line mixing (---), with line mixing (—) and the experimental values (■). The pressure of  $\text{N}_2$  gas increases from left panel to right. The lower panels correspond to residuals of the fits showing the differences between the experimental spectra and calculated one using a sum of Lorentz profiles with (last panel) or without (first residual panel) taking into account line-mixing effects.



\*  $^RQ_9$  branch of the  $\nu_4$  band taken into account in the calculation of the total absorption coefficient (Lorentz profiles). Spectroscopic data of these transitions are less accurate than the  $\nu_1$  ones.

Figure 5

Comparison between the  $\text{CH}_3\text{Cl}/\text{N}_2$  PNNL experimental spectra (■) of the  $^oQ$  sub-branch and those calculated without line mixing (---), with line mixing (—).  $P(\text{CH}_3\text{Cl}) = 1.10^{-6}$  atm,  $P(\text{N}_2) = 1$  atm,  $L = 100$  cm (experimental conditions from PNNL [22]). The panels of residuals show the differences between the experimental PNNL spectrum and a calculation without taking into account line-mixing effects (a) and by using our model to model line-mixing effects (b).

